

SDQM: Synthetic Data Quality Metric for Object Detection Dataset Evaluation

Ayush Zenith^a, Arnold Zumbun^b, Neel Raut^a, Jing Lin^c

^aKhoury College of Computer Sciences, Northeastern University, Boston, MA, USA

^bSchool of Computing, Binghamton University, Binghamton, NY, USA

^cMission Applications & Infrastructure Section, Air Force Research Laboratory, Rome, NY, USA

Abstract. The performance of machine learning models depends heavily on training data. The scarcity of large-scale, well-annotated datasets poses significant challenges in creating robust models. To address this, synthetic data generated through simulations and generative models has emerged as a promising solution, enhancing dataset diversity and improving the performance, reliability, and resilience of models. However, evaluating the quality of this generated data requires an effective metric. This paper introduces the Synthetic Dataset Quality Metric (SDQM) to assess data quality for object detection tasks without requiring model training to converge. This metric enables more efficient generation and selection of synthetic datasets, addressing a key challenge in resource-constrained object detection tasks. In our experiments, SDQM demonstrated a strong correlation with the mean Average Precision (mAP) scores of YOLOv11, a leading object detection model, while previous metrics only exhibited moderate or weak correlations. Additionally, it provides actionable insights for improving dataset quality, minimizing the need for costly iterative training. This scalable and efficient metric sets a new standard for evaluating synthetic data. The code for SDQM is available at <https://github.com/ayushzenith/SDQM>.

Keywords: synthetic data, dataset quality, object detection, evaluation metric, model performance.

1 Introduction

There is an increased interest in creating synthetic data to address the data challenges, particularly in domains where collecting and labeling real-world data is expensive and time-consuming. Synthetic data can be generated from various sources, including digital data (e.g., images or videos) produced by physics-based simulated 3D environments or through generative AI. In this paper, we focus on simulation-based synthetic data due to its advantages in physical accuracy, reproducibility, traceability, explainability, and configurability.

However, bridging the gap between synthetic and real data typically involves multiple rounds of testing and refinement. This iterative process is essential to ensure that the synthetic data accurately reflects the characteristics and variability of real-world data, making it useful for training models. Despite the potential benefits, the resources required for effective synthetic data gen-

eration, combined with the need for repeated testing and fine-tuning, pose major hurdles to its widespread adoption.

We aim to develop an integrated metric — a mathematical formula that combines one or more individual metrics or properties — to assess the usefulness of synthetic datasets for object detection. The key idea is that a higher score on our SDQM metric will correlate with improved model performance when the object detection model is trained on that dataset. This would provide a cost-effective and efficient predictive measure of the dataset’s effectiveness, allowing for an estimation of how well a model would perform without the need for exhaustive training and testing.

Although this paper is primarily focused on object detection, this metric could be extended to similar tasks including instance segmentation, object localization, and image classification. Furthermore, as a dataset quality metric, it would serve as a useful benchmark for future research involving the creation of mixed real and synthetic datasets. In summary, our key contributions are as follows:

- We explore various existing data quality metrics for generative AI models and investigate their effect on predicting the performance of object detection models trained on synthetic data.
- We develop a data quality metric, SDQM, for object detection by evaluating the pixel space, spatial space, frequency space, and feature space domain gap using both state-of-the-art AI techniques and various non-parametric distribution comparison techniques.
- We validate the effectiveness of SDQM, demonstrating a strong correlation ($r = 0.87$) between SDQM values and model performance (i.e., mAP50 scores of object detection models trained on synthetic data). The metric’s predictive capability reduces reliance on exhaustive

training-validation cycles, as shown by consistent performance gains across multiple diverse datasets such as RarePlanes,¹ Dataset of Industrial Metal Objects (DIMO),² and WASABI.³

2 Related work

Dataset quality has been studied in different contexts, emphasizing data quality metrics and dataset interpretability. In this section, we provide a brief review of the relevant metrics and research on dataset interpretability.

2.1 Existing Data Quality Metrics

There exist several approaches to establishing a data metric. Structured Similarity Index Metric (SSIM, MSSIM)⁴ was developed to assess the similarity between images by considering changes in structural information. This metric is widely used in image quality assessment. However, this metric is content invariant and thus will not be particularly helpful in comparing the collections of real and synthetic images for the proposed use case. Similarly, Zhang et al.⁵ designed Learned Perceptual Image Patch Similarity (LPIPS) to measure the perceptual similarity between images based on deep network features. While it is useful for comparing the quality of synthetic images with their real counterparts, it is again content-invariant and not helpful in determining the usefulness of images for training an object detection model.

One of the earliest data quality evaluation metrics for GANs is the Inception score (IS).⁶ IS assesses the quality of generated images based on the output probabilities of a pre-trained Inception v3 model. Higher scores indicate data are both diverse and recognizable as real objects. However, the metric is biased toward images that resemble those on which the Inception model was trained, and it does not consider the statistics of real-world samples. To improve it, Fréchet Inception

Distance (FID)⁷ was later introduced to incorporate the statistics of real-world samples to quantify the difference between the feature distributions of real and generated images. Lower FID scores suggest a higher similarity between these distributions. Various FID variants exist, each with its own drawbacks, as discussed in Ref. 8.

Recently, MAUVE⁹ evaluates the similarity between a real and a synthetic data distribution using quantized embeddings and divergence measures. It has shown promise in evaluating the quality of generative data in natural language processing, and by adapting it for image data, it has earned its place as one of the sub-metrics included in the calculation of SDQM. Generative Precision and Recall¹⁰ provide a more nuanced evaluation of generative models by measuring the fidelity and diversity of generated samples, although MAUVE seems to outperform these metrics when it comes to comparing two distributions in the generative evaluation space. Alaa et al.¹¹ improved the Generative Precision and Recall metrics by designing the α -Precision, β -Recall, and Authenticity metrics to measure fidelity, diversity, and authenticity, respectively.

- α -Precision:¹¹ Determines the extent to which synthetic data aligns with the dense regions of the real data distribution. High α -Precision ensures the dataset includes realistic and plausible samples without focusing excessively on outliers or edge cases.
- β -Recall:¹¹ Measures the diversity of synthetic data by evaluating the fraction of real data distribution covered by the generative model. High β -Recall implies that the synthetic dataset is capturing a broad range of modes from the real data, avoiding mode collapse or narrow sampling.
- Authenticity:¹¹ Assesses the novelty of synthetic samples by determining how many of them are unique and not near duplicates or direct copies of real training data. High Authenticity

indicates the synthetic dataset is capable of generating genuinely new and diverse samples.

These individual metrics, while valuable, cannot address the complexities of evaluating data and are incapable of metricizing quality, which we define as a direct correlation of model performance.

2.2 Dataset Interpretability

The previously mentioned metrics focus primarily on evaluating data quality through data distributions. Dataset Interpretability, however, involves assessing the value of individual data points or subsets within a larger dataset, identifying which specific points or subsets most contribute to improving model performance. The concept of \mathcal{V} -Usable Information¹² quantifies the useful information a dataset provides for a specific task, offering a way to assess dataset difficulty (how challenging it is for a model to learn from it). We draw upon the framework introduced by Ethayarajh et al.¹² to incorporate Dataset Interpretability into our metric. Data Maps¹³ is another proposed technique to analyze training dynamics and categorize data points based on their difficulty and consistency. This method provides valuable insights into dataset quality and helps identify problematic examples that may hinder model training.

Together, these related works lay a solid foundation for developing a comprehensive dataset quality metric tailored to synthetic data in object detection tasks. They also establish benchmarks against which our proposed metrics can be compared. By extending and integrating these existing methods, we aim to create a robust metric that not only quantifies dataset quality but also guides the generation of high-quality synthetic datasets.

3 Methodology

SDQM consists of several independent components (or sub-metrics), each made up of one or more sub-components that measure specific attributes — such as quality, fidelity, or distribution alignment — of object detection datasets. As shown in Sec. 2, existing metrics mainly focus on evaluating data quality or distribution alignment but lack emphasis on the usefulness of the images for object detection model training. In this section, we present our methodology for developing SDQM that quantifies the dataset’s effectiveness for training object-detection models using both existing metrics and various non-parametric distribution comparison techniques.

3.1 Individual Metrics for Dataset Quality Evaluation

We begin by reviewing existing data quality metrics and assessing their impact on predicting the performance of object detection models trained on synthetic data. We then select a range of established metrics and propose new methods for calculating additional metrics that complement the existing ones.

As described in Sec. 2, MAUVE computes the area under the curve of the Kullback-Leibler (KL) divergence frontier of the quantized distributions of embeddings from real and synthetic datasets, whereas Frontier Integral (FI) provides a summary of the statistics related to the divergence frontiers discussed in Ref. 14. Pillutla et al.⁹ introduced two versions of MAUVE, which are both combined to make SDQM’s MAUVE component using quadratic analysis. Similarly, two versions of FI are combined. For details, please see the technical appendix. Figure 1 shows the moderate correlation with mAP50 (last column) of the components. Notably, the strong correlation between MAUVE and FI (likely stemming from the fact that they measure similar characteristics) indicates that we may not need both of them.

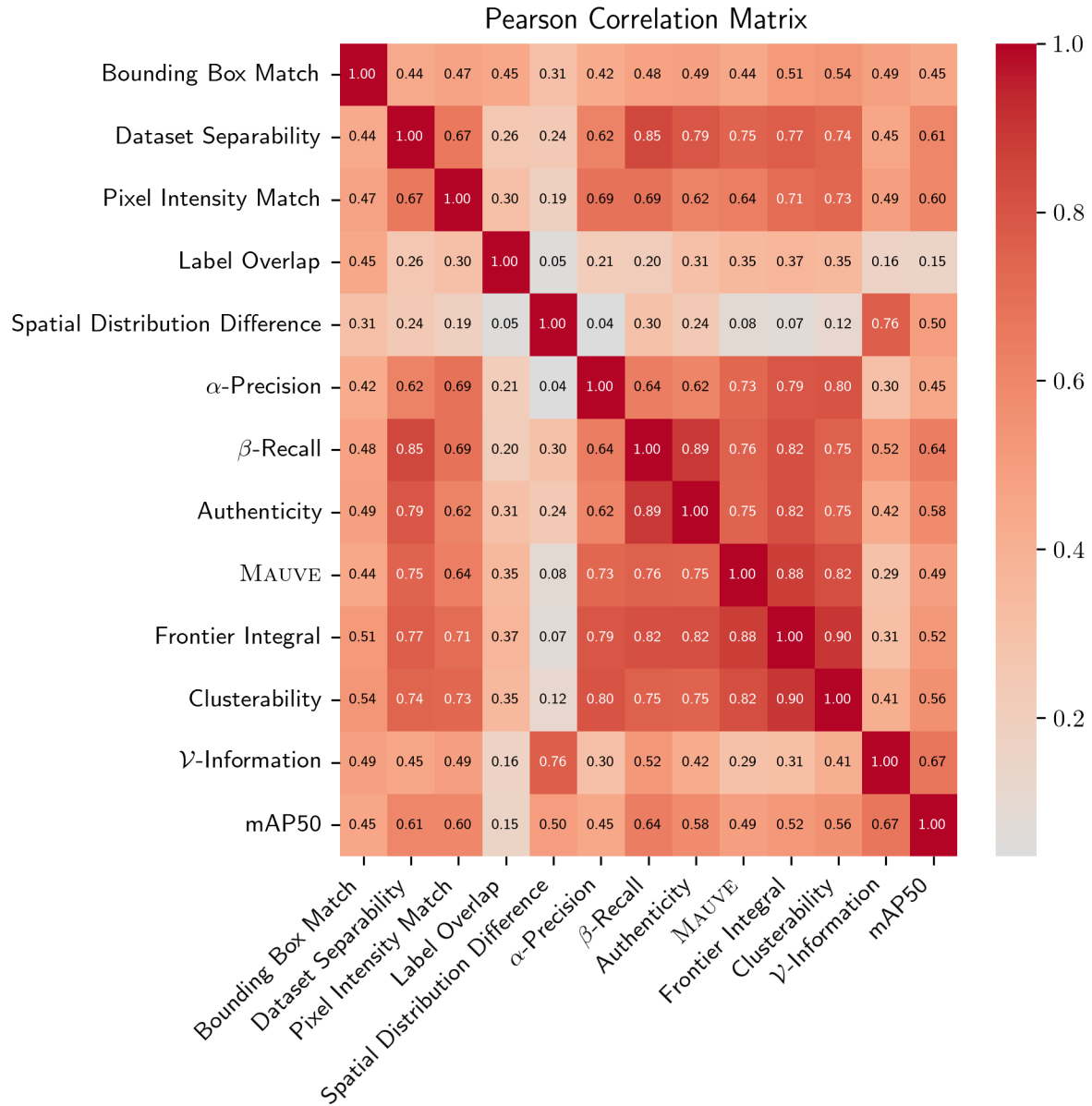


Fig 1 Correlation between each sub-metric and mAP50.

To ensure that the synthetic dataset is diverse, realistic, and not overly repetitive, α -Precision, β -Recall, and Authenticity are also taken into account. Figure 1 illustrates the correlation (all ≥ 0.62) among these metrics, demonstrating the interconnection between the metrics. We will later analyze these metrics to explore better integration methods for higher correlation with mAP50.

Although these metrics are suitable for our purpose, each has limitations. We propose two

additional metrics — Dataset Separability and Clusterability — to better assess synthetic data embedding space overlap. The Dataset Separability component utilizes AutoKeras¹⁵ to choose a neural network architecture and train the network to classify embeddings as real or synthetic. To measure the level of ease with which the model separated the real and synthetic embeddings, we record the evaluation accuracy of the highest-performing model. Theoretically, a sufficiently complex model can separate any set of real and synthetic embeddings with a high evaluation accuracy; therefore, a model’s evaluation accuracy must be juxtaposed with its complexity for an accurate measure of dataset separability. To keep track of the balance between effectiveness and efficiency, we record the parameter count of the model selected by AutoKeras in addition to its evaluation accuracy. These two measures are weighted appropriately along with other metrics in Sec. 3.3.

To assess Clusterability, we employ the k -means clustering algorithm to jointly cluster the real and synthetic embeddings. The log cluster metric equation,

$$LC(R, S) = \log \left(\frac{1}{k} \sum_{i=1}^k \left[\frac{n_i^R}{n_i} - \frac{n^R}{n} \right]^2 \right), \quad (1)$$

accentuates smaller differences between the data points, where k is the number of clusters, n is the dataset size, n^R is the total number of real images, n_i is the total number of data points assigned to cluster i , and n_i^R is the number of real data points assigned to cluster i . In simpler terms, we compute the average of the squared differences between the actual proportion of real data points in each cluster and the expected proportion of real images across all clusters. If the clusters are inseparable, the expected proportion is $\frac{n^R}{n}$. Figure 1 shows that Dataset Separability and Clusterability each correlate moderately with mAP50; furthermore, the two components themselves correlate strongly with each other and certain other components. Section 3.3 further investigates this.

To evaluate the objects and characteristics in the synthetic dataset, we quantify the Label Overlap between synthetic and real imagery. Using the annotations and metadata of real and synthetic datasets, we can create probability distributions for each and use probability distribution comparison metrics, i.e., the Kolmogorov-Smirnov (K-S) test,¹⁶ Anderson-Darling (A-D) test,¹⁷ Kullback-Leibler (KL) divergence,¹⁸ Energy Distance (ED),¹⁹ Wasserstein Distance (WD),²⁰ Bhattacharyya Distance (BD),²¹ and Jensen-Shannon (JS) Divergence.²² Section 3.3 provides an analysis of the effectiveness of each of these metrics. In all cases, we create a probability distribution based on the number and category of objects in an image; furthermore, in the case of a dataset containing informative metadata about images — such as the weather condition, biome, or physical location — we factor the additional metadata into the distribution used for comparison.

Spatial Distribution Difference compares the distributions of objects in the real imagery and its synthetic counterpart. The more similar the spatial distribution of synthetic data is to real data, the lower the spatial distribution score will be. We calculate the spatial distribution score by initializing a spatial distribution heatmap as a matrix of size $w \times h$ for each dataset, where w is the image width and h is the image height. Each position in the matrix is incremented by one for each object that overlaps with the pixel corresponding to that position. The real heatmap is then compared with the synthetic heatmap using root mean squared error (RMSE). Before the RMSE operation, a mean pooling operation reduces the size of the heatmap by a factor of eight; the pooling forces RMSE to work on a more global scale and adds smaller penalties for more localized differences.

Furthermore, by comparing aspect ratios, diagonal lengths, and areas of bounding boxes, we form a complete picture of the types of bounding boxes in each dataset and calculate a Bounding Box Match score using the following nonparametric statistical tests: Kolmogorov-Smirnov (K-S), Anderson-Darling (A-D), Kullback-Leibler (KL) divergence, Energy Distance (ED), Wasserstein

Distance (WD), Bhattacharyya Distance (BD), and Jensen-Shannon (JS) Divergence.

We then analyze the pixel intensity in all images. Comparing the overall pixel intensity distributions of the synthetic and real datasets, we derive our Pixel Intensity Match component. To ensure that the intensity of pixels across all three color channels (red, green, blue) in synthetic data is similar to that in real data, we calculate the distributions of pixel values for each channel in each image and then run the non-parametric statistical tests as listed previously.

Lastly, we calculate and metricize the interpretability of the synthetic dataset by accounting for the object detection model family \mathcal{V} . We use the foundation laid in \mathcal{V} -Usable Information¹² and extend it for object detection models. We call our extension simply \mathcal{V} -Information, which measures the difficulty of the dataset by analyzing how easily a model can learn from the synthetic data and apply it to the target domain. This will help us understand how to close the domain gap. The \mathcal{V} -Information equation is

$$I_V(X \rightarrow Y) = H_V(Y) - H_V(Y|X). \quad (2)$$

To calculate the conditional and predictive entropy H_V for the above described variants in an efficient manner on the YOLOv11²³ family, the following implementation is employed:

- Conditional Entropy is defined as

$$H_V(Y | X) = \inf_{f \in \mathcal{V}} \mathbb{E} [-\log_2 f[X](Y)]. \quad (3)$$

To compute the conditional entropy, we fine-tuned a model, in our case the pre-trained YOLOv11n checkpoint, on the synthetic dataset, while freezing the backbone layers for

E epochs, ensuring the number of epochs was greater than the warm-up phase yet still kept relatively low. We opted for YOLOv11n as it strikes an optimal balance between minimizing computation time and allowing us to effectively assess the model’s performance and knowledge before and after training. In our experiments, YOLOv11n was trained for $E = 10$ epochs before validation on the real dataset, during which we calculated the conditional entropy.

- Predictive Entropy is defined as

$$H_{\mathcal{V}}(Y) = \inf_{f \in \mathcal{V}} \mathbb{E}[-\log_2 f[\emptyset](Y)]. \quad (4)$$

To calculate the predictive entropy, we use the pre-trained YOLOv11n model, which has been trained on the COCO dataset,²⁴ and validate its performance on a real dataset. During the validation process, the model’s predictions are matched with the corresponding annotation classes in the real dataset. For example, in the RarePlanes dataset, class 0 represents ‘airplane’, while in COCO, class 5 represents ‘airplane’. Thus, any prediction made by the model that corresponds to class 5 is compared with the annotation label of class 0, and all other predictions are ignored. The predictive entropy is then calculated based on this validation process.

As shown in Fig. 1, our extended \mathcal{V} -Information exhibits the strongest individual correlation with mAP50 compared to all others discussed. We will further improve it to obtain the SDQM metric. Notably, the MAUVE, FI Score, Clusterability, \mathcal{V} -Information, α -Precision, β -Recall, and Authenticity metrics all require embeddings extracted from images to work effectively. Next, we

outline the process of selecting the feature extraction model.

3.2 Evaluating Feature Extraction Models

Feature extraction forms the backbone of many metrics. To obtain optimal results, selecting a high-quality model for feature extraction is crucial. Below are the feature extractors we have chosen for further exploration and evaluation.

1. DinoV2-small:²⁵ A robust vision transformer trained using self-supervised learning methods. Known for its strong performance, DinoV2-small excels at capturing and extracting semantic features across diverse datasets, all without the need for labeled data, outputting features in 384 dimensions.
2. GroundingDINO-tiny:²⁶ A compact version of GroundingDINO designed for efficient open-set object detection with grounding capabilities, making it well-suited for tasks requiring feature alignment between real and synthetic data. The model was modified to use only the encoder, which takes in an image and a text prompt and outputs features in 256 dimensions.
3. CLIP-ViT-B/32:²⁷ A vision transformer pretrained, using contrastive learning, on a large set of image-text pairs. It is particularly effective for zero-shot tasks and generalizing across domains. As a multi-modal model, CLIP encodes images and text into a single embedding space. The ViT-B/32 variant divides images into 32x32 patches and processes them through a transformer, outputting feature embeddings in 512 dimensions.

By “feature extractor quality,” we refer to a model’s ability to transform raw images into information useful for downstream tasks, such as object detection and image classification. We hypothesize that the effectiveness of a feature extraction model is reflected in how easily it allows

computational methods to reconstruct human-defined characteristics of the original dataset. To assess model quality, we leverage known, human-labeled attributes of the raw data for evaluation.

We evaluate feature extractor quality using the DIMO dataset, which provides real and synthetic image pairs. The dataset features objects with varying shapes and angles in a controlled environment, making it ideal for assessing feature extraction performance. For each real-synthetic pair, we compute cosine similarity and Euclidean distance between the feature representations produced by different models. The models are ranked based on their average and cumulative performance across all pairs. The model with the highest average cosine similarity, lowest average Euclidean distance, and best overall cumulative scores is selected as the most effective feature extractor for preserving the fidelity between real and synthetic data.

Among the three feature extractors, the GroundingDino-tiny model achieved the best performance in feature extraction based on the methodology described above. This evaluation demonstrates the model's ability to consistently capture meaningful features across the diverse conditions present in the DIMO dataset. For a detailed overview of the results, refer to the technical appendix.

3.3 SDQM: Integrated Metric Development

We perform a correlation analysis to group the sub-components of each sub-metric and eliminate those with limited informational value, helping streamline the metric development process. After conducting an exploratory study to combine the sub-components of each sub-metric and analyzing their relationship with mAP50, we determine that random forest regression best fits the data (detailed further in the technical appendix). This method effectively handles multivariate dependencies and identifies the most influential components, which we discuss further in this section.

The Bounding Box Match, Pixel Intensity Match, and Label Overlap components each com-

prise a set of nonparametric statistical tests; therefore, we analyze the contributions of each of these tests to the performance of each sub-metric and select the best performing statistical test for each sub-metric, i.e., A-D Statistic for Pixel Intensity Match, Energy Distance for Bounding Box Match, and K-S Statistic for Label Overlap.

For each of the other components, we conduct multivariate regression using a combination of linear, quadratic, and interaction terms to examine their interrelationships. The selection of terms is based on p-values from the regression results. For example, in the Dataset Separability component, which has the number of parameters (p) and validation accuracy (a) as sub-components, the resulting regression analysis assigns a negative weight to a and a positive weight to p . This reflects the notion that synthetic data becomes easier to distinguish from real data as a increases with the same p , but harder to separate when p is lower with the same a . This establishes a positive correlation between Dataset Separability and mAP50, where higher values of the Dataset Separability component indicate greater difficulty in distinguishing synthetic data from real data.

To illustrate how the sub-metrics relate to each other and the performance of the empirical model, the correlation matrix in Fig. 1 was created using data points obtained using the method described in Sec. 4. Observing that MAUVE correlates highly with Frontier Integral, Authenticity correlates highly with β -Recall, and Clusterability correlates highly with FI and MAUVE, we ran the backward feature reduction method²⁸ on the data and confirmed that the removal of MAUVE, Authenticity, and Clusterability does not reduce linear regression performance and only slightly reduces random forest performance. We remove these three sub-metrics from the data before proceeding with the regression analysis in Sec. 4.

Figure 1 indicates that the sub-metrics with the highest correlation with the empirical model performance are \mathcal{V} -Information, β -Recall, Dataset Separability, and Pixel Intensity Match. Label

Overlap correlated the least with model performance. The correlations between each of our selected sub-metrics and mAP50 provide valuable insights into their effectiveness and intimate certain characteristics of object detection models. For example, the weak correlation between Label Overlap and mAP50 indicates that YOLOv11 can effectively learn to disregard variations in object counts and certain other annotation attributes within datasets. Conversely, the high correlation of the Pixel Intensity Match sub-metric emphasizes its importance in synthetic-real domain gap analysis. Additionally, embedding space sub-metrics (i.e., Dataset Separability, α -Precision, β -Recall, Authenticity, MAUVE, FI, and Clusterability) exhibited a high correlation with the model performance, suggesting the embedding models used in preserving important information about images and the sub-metrics that perform embedding space comparisons effectively distinguish real from synthetic data. Finally, our \mathcal{V} -Information sub-metric, which shows the strongest correlation with model performance, underscores its importance in evaluating the usefulness of a dataset for training. These sub-metrics are integrated using a random forest, resulting in the proposed metric. Detailed information is provided in Sec. 4.

4 Experiments

This section presents extensive experiments to validate the proposed metric, investigating its correlation with the model performance. To ensure robust verification, we collect a large number of data points by employing an evolutionary algorithm to select subsets from three synthetic-real dataset pairs. This robust methodology enables a thorough evaluation of the metric's effectiveness across various challenging scenarios, enhancing its validity and practical applicability.

- Rareplanes¹ – a large-scale collection of real and synthetic overhead imagery specifically designed to evaluate the effectiveness of synthetic data in training object detection models.

It includes high-quality annotations with a variety of features and characteristics, making it an excellent resource for studying synthetic data generation methods and assessing their impact on model performance. The dataset includes

- 130 different real locations and fifteen synthetic locations
 - Five distinct synthetic biomes: alpine, arctic, temperate evergreen forests, grasslands, and tundra
 - Weather information for real and synthetic data
 - Other information such as sunlight intensity, time of day, camera angles, and real world dates and times
- Dataset of Industrial Metal Objects (DIMO)² – a high-resolution collection designed to advance research in object detection, including evaluating the impact of synthetic variations on model generalization. The dataset consists of:
 - Real-world Data: 31,200 images from 600 scenes
 - Synthetic Data: Generated using Unity, the dataset includes 553,800 images across 42,600 scenes. The synthetic data in the DIMO dataset replicates real-world lighting, object poses, and textures. Textures are designed to simulate real-world effects, such as scratches, using texture synthesis algorithms.
 - WASABI³ – an overhead collection featuring various vehicle and personnel labels. This research centers exclusively on vehicle detection. The dataset comprises about 100,000 real images from 519 videos, with object count distribution illustrated in Fig. 2. It also features a synthetic collection of over 20,000 images, preserving the resolution of the original images.

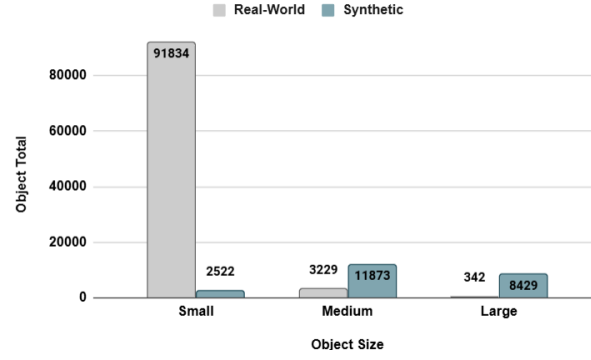


Fig 2 WASABI object size and count. Note: “Small,” “Medium,” and “Large” definitions are based on Ref. 24.

Dataset Partitioning. Before running the evolutionary algorithm, we divide the real and synthetic data into separate training, evaluation, and test splits, ensuring that each split contains distinct real and synthetic scenes. Then, we execute Algorithm 1 for each split. First, we apply an evolutionary algorithm²⁹ to select subset pairs with varying similarity. For each sub-metric m outlined in Sec. 3.1 and for each of the n values equally spaced across the range of m_j , i.e., $L = \{m_j : m_{j+1} - m_j = m_j - m_{j-1}\}_{j=1}^n$, we execute the algorithm. The fitness function calculates the difference between the sub-metric value of an individual in the population and the current sub-metric value we are optimizing for. In other words, an individual’s fitness increases as the subset pair it represents moves closer to the target sub-metric value.

Additionally, a penalty, described in Algorithm 1, is applied based on how much the subset sizes deviate from the desired range. We use early stopping when the fitness function reaches a value below 0.005. After discovering that the algorithm struggled to converge for sub-metrics other than α -Precision, β -Recall, and Authenticity, we are left with these three sub-metrics for dataset selection. In total, we use three embedding models, three sub-metrics, and 11 equally spaced values between 0 and 1 for each sub-metric to ensure diverse sets are selected for the experiments. This process results in 364 training subsets and 64 evaluation subsets for use in the regression. For details, please refer to Algorithm 1. Table 1 provides descriptions of notations and symbols

Algorithm 1 Dataset selection

```
1: Input:  $\mathcal{X}, \mathcal{X}', k_l, k_u, \phi, g, n, P_m, P_c$ , and  $s$ 
2:  $\Phi = \varphi(\mathcal{X}) \cup \varphi(\mathcal{X}')$ 
3: for  $m \in \mathcal{M}$  do
4:   Select  $n$  values equally spaced across the range of  $m$ , i.e.,  $L = \{m_j : m_{j+1} - m_j = m_j - m_{j-1}\}_{j=1}^n$ 
5:   for  $m_j \in L$  do
6:      $\mathcal{P} = \emptyset$ .
7:     for  $i = 1$  to  $p$  do
8:       Randomly select  $s_1^i, s_2^i \in [k_l, k_u]$ .
9:       Randomly generate  $D^i = (D_1^i, D_2^i)$  such that  $D_1^i, D_2^i \subset \Phi$ ,  $D_1^i \cap D_2^i = \emptyset$ ,  $|D_1^i| = s_1^i$ , and  $|D_2^i| = s_2^i$ 
10:       $\mathcal{P} = \mathcal{P} \cup D^i$ 
11:       $f(D^i, m, m_j) = |m_j - m(D^i)| +$   


$$\frac{\text{dist}(k_l, k_u, |D_1^i|) + \text{dist}(k_l, k_u, |D_2^i|)}{\max(k_u - k_l, 1)} \cdot \text{Range}(m)$$

12:    end for
13:    for each generation do
14:      if the minimum individual fitness in the population is less than 0.005 then
15:        Select the individual with this fitness.
16:        Continue to the  $m_{j+1}$ .
17:      end if
18:      Create offspring  $D$  from the population using crossover with probability  $P_c$  and mutation with probability  $P_m$ 
19:      Evaluate  $f(D, m, m_j)$ 
20:    end for
21:    if no individual has been selected then
22:      Select the individual with the minimum fitness
23:    end if
24:  end for
25: end for
```

Algorithm 1.

Model Training. For each selected subset pair, a YOLOv11n model trains on one dataset for ten epochs and evaluates on a randomly selected subset of the real test data. In our experiment, YOLOv11n reached mAP50 values between 0.31 and 0.79 in the training data and 0.06 and 0.40 in the evaluation data when trained on the uniformly sized, evolutionarily selected subsets. The

Table 1 Description of all parameters, functions, and variables in Algorithm 1.

PARAMETER	DESCRIPTION
\mathcal{X}	Images from real dataset
\mathcal{X}'	Images from synthetic dataset
k_l, k_u	Lower and upper bounds for subset size
g	Number of generations
n	Number of values to optimize for
p	Population size
P_m	Mutation probability
P_c	Crossover probability
s	Stopping criteria
$\text{dist}(a, b, c)$	Distance of c outside $[a, b]$. If c is within $[a, b]$, then $\text{dist}(a, b, c) = 0$
	$\text{dist}(a, b, c) = \begin{cases} c - a, & \text{if } c < a \\ c - b, & \text{if } c > b \\ 0, & \text{otherwise} \end{cases}$
φ	Embedding model
\mathcal{M}	Set of metrics to use

discrepancy between the training and evaluation performance exemplifies the domain gap between the synthetic and real-world data. To both extend the range of mAP50 values covered by the evaluation data and add diversity to the sizes of the subsets, additional subsets were randomly selected. Random real subsets and random synthetic subsets were paired along with real test data to extend the range of mAP50 values to fall between 0.06 and 0.79 for the evaluation data.

SDQM Development. After the above procedures, a regression can be performed with the sub-metric values between a subset pair as inputs and the mAP50 score of the respective YOLOv11n model as the output. These values for each dataset pair are collected and shuffled before splitting into train and evaluation sets. K-fold cross-validation could be performed to assess the correla-

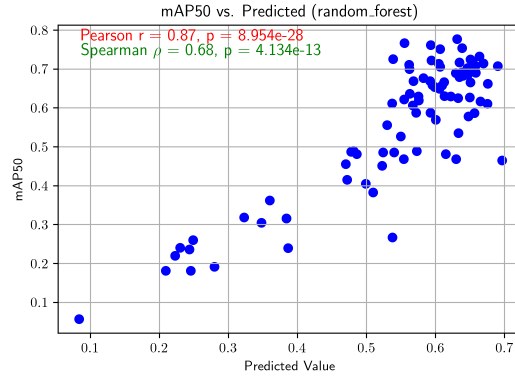


Fig 3 Validation datapoints with SDQM values calculated from random forest coefficients vs. YOLOv11n mAP50 scores.

tion variation due to the randomness in the splitting process. A sample result from a random train split and a random evaluation split is presented in Fig. 3; the trial yielded a Pearson correlation coefficient of 0.82 and a Spearman correlation coefficient of 0.65 on the evaluation split. Furthermore, taking the mean across each of the 10 correlation coefficients in the k-fold cross-validation procedure, the result is a Pearson coefficient of 0.78 with a standard deviation of 0.091 and Spearman coefficient of 0.58 with a standard deviation of 0.14. This result indicates consistency in the regression across the random splits. Finally, the highest weighted metrics the regression analysis found to be most important were Pixel Intensity Analysis, β -Recall, and \mathcal{V} -info.

Since the idea of a comprehensive synthetic data evaluation metric is novel, the closest metrics we can compare with SDQM to evaluate performance would be existing generative model evaluation methods. Table 2 presents this comparison in the context of our subset selection and YOLOv11 model training procedure. SDQM, our metric, surpasses all other metrics in terms of Pearson correlation with mAP50. Based on common correlation strength thresholds, SDQM is strongly correlated with mAP50 while other metrics are moderately correlated at best.

Table 2 Correlation of alternative metrics and SDQM with mAP50 scores.

Metric	mAP50
Pearson Correlation	
α -Precision ¹¹	0.4477
β -Recall ¹¹	0.5865
Authenticity ¹¹	-0.3482
MAUVE ⁹	0.5651
SDQM (ours)	0.8719

5 Conclusion

In conclusion, SDQM provides a simple approach to evaluating synthetic dataset quality for object detection tasks. By combining multiple sub-metrics and sub-components that address critical aspects of dataset quality — including coverage, diversity, domain similarity, and interpretability — SDQM predicts the efficacy of synthetic datasets in improving model performance. This reduces the reliance on extensive and computationally expensive training-validation cycles. Our work provides greater insight into the interpretability of object detection models, and the results demonstrate that SDQM strongly correlates with mAP scores of models trained on synthetic data and validated on real-world datasets. The high correlation of SDQM shown in Fig. 3, compared to the lower individual sub-metric correlations in Fig. 1, further emphasizes the need for our integrated metric. This predictive capability enables more efficient dataset selection and generation, especially in resource-constrained scenarios, and improves the scalability of synthetic data usage in object detection.

Appendix A: Feature Extraction Evaluation

To assess the feature extraction capabilities of different models, we evaluated the cosine similarity and Euclidean distance between feature representations of synthetic and real pairs from the DIMO dataset as described in the SDQM paper. Cosine similarity measures the angular closeness

between two vectors, where values closer to 1 indicate higher similarity. In contrast, Euclidean distance quantifies the absolute difference in feature space, with smaller values representing greater proximity between features. These metrics provide complementary insights into how well a model preserves semantic and spatial consistency across synthetic and real data.

Table 3 presents the evaluation results for three models: GroundingDino-tiny, CLIP-ViT-B/32, and DinoV2-small. The models differ significantly in their ability to maintain consistency between synthetic and real data, as evidenced by variations in cosine similarity and Euclidean distance statistics. As per our findings below, GroundingDino-tiny encoder seems to provide us with the best features for our use case.

Table 3 Feature extraction model evaluation report.

Model	Cos Sim Sum	Mean Cos Sim	Euc. Dist. Sum	Mean Euc. Dist.
GroundingDino-tiny	7707.237835	0.989757	760.091262	0.097610
CLIP-ViT-B/32	6949.146740	0.892404	40393.930023	5.187355
DinoV2-small	6566.421186	0.843254	129133.357791	16.583197

Appendix B: Existing Sub-Metric Evaluation: α -Precision, β -Recall, and Authenticity

The results presented in Table 4 highlight the α -Precision, β -Recall, and Authenticity scores for different datasets when evaluated using three models: DinoV2, Grounding-Dino, and ViT. These metrics are crucial for understanding how well synthetic and real datasets perform in terms of precision, recall, and authenticity when paired with different models.

For our datasets, α -Precision varied the most out of the three metrics. DIMO and its synthetic counterpart had the highest α -Precision scores, suggesting the synthetic counterpart matched the real data distribution well. β -Recall, being low for all tests, suggests that a significant portion of the real data fell outside of the synthetic data distributions for our dataset. Finally, as expected

since our synthetic datasets are all physics-based, Authenticity indicates synthetic datapoints were not “stolen” from real datapoints.

Table 4 α -Precision, β -Recall, and Authenticity scores of the various synthetic and real-world dataset pairs.

Dataset	Model	α -Precision	β -Recall	Authenticity
DIMO	DinoV2	0.394860	0.051795	0.996389
DIMO	Grounding-Dino	0.827369	0.182025	0.983838
DIMO	ViT	0.682937	0.001035	0.997654
DIMO-Counterpart	DinoV2	0.602352	0.029452	0.947220
DIMO-Counterpart	Grounding-Dino	0.938879	0.078241	0.902401
DIMO-Counterpart	ViT	0.776746	0	0.979068
WASABI	DinoV2	0.149050	0	1
WASABI	Grounding-Dino	0.087010	0	1
WASABI	ViT	0.041659	0	1
RarePlanes	DinoV2	0.416685	0	0.997577
RarePlanes	Grounding-Dino	0.683583	0.185365	0.921733
RarePlanes	ViT	0.466974	0	0.985980

Appendix C: Existing Sub-Metric Evaluation: MAUVE, FI, MAUVE*, and FI*

Table 5 shows MAUVE and FI scores as well as the smoothed scores (indicated by *) for different synthetic and real dataset pairs using different feature extractors. As shown, the scores change with the selection of different feature extractors. The dependency in scores is why the choice of feature extractor is crucial when evaluating the similarity between datasets using metrics like MAUVE and FI. As observed, feature extractors such as DinoV2-small, CLIP-ViT-B/32, and GroundingDino-tiny produce varying scores for the same dataset pairs. This variability highlights the sensitivity of these metrics to the underlying representations of the data provided by different models. Consequently, this emphasizes the need for careful selection of feature extractors tailored to the specific characteristics of the datasets being compared, as well as the importance of standardizing evaluation pipelines to ensure consistent and reliable comparisons.

Key for Table: RP=‘RarePlanes’, GD=‘GroundingDino-tiny’, W=‘WASABI’, R=‘Real’,

Synth='Synthetic', Tr='Train', Val='Validation'

Appendix D: Comparison of Regression Methods

As the random forest regression method yielded the best correlation result for our data, we chose to display it in Section the main paper. In addition, we present the results of five other regression methods: decision tree (Fig. 7), lasso (Fig. 8), linear (Fig. 4), XGBoost (Fig. 6), and ridge (Fig. 5). Interestingly, all of these methods, with the exception of lasso regression, reach Pearson correlation coefficients within 0.05 of random forest.

Figure 4 displays predictions using linear regression. Attesting to the robustness of SDQM's underlying sub-metrics, this simple linear regression model still performed well on our data. For this reason, one may choose to use linear regression to calculate SDQM if one desires a simpler model.

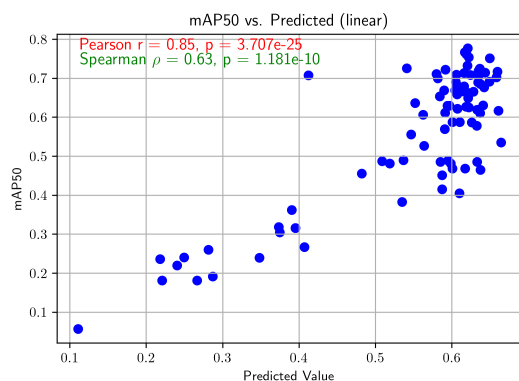


Fig 4 Validation datapoints with SDQM values calculated from linear regression coefficients vs. YOLOv11n mAP50 scores.

Figure 5 displays ridge regression results. The performance of ridge regression, linear regression with an L2 regularization term, achieves the same performance as standard linear regression.

Figure 6 displays the performance of xgboost. This regression method achieved the same Spearman correlation coefficient as random forest and a Pearson correlation coefficient only 0.01

Table 5 MAUVE and Frontier Integral scores (along with smoothed variants indicated by *) of the various synthetic and real-world dataset pairs.

Model	Dataset P	Dataset Q	MAUVE	MAUVE*	FI	FI*
DinoV2-small	RP: R Tr	RP: R Val	0.610339	0.662745	0.158725	0.140987
DinoV2-small	RP: R Tr	RP: Synth	0.010485	0.020507	0.846375	0.734662
DinoV2-small	W: R Tr	W: R Val	0.008292	0.017457	0.886670	0.761341
DinoV2-small	W: R Tr	W: Synth	0.004073	0.009237	0.999945	0.862455
DinoV2-small	DIMO: R	DIMO: Synth	0.057809	0.093659	0.573631	0.491431
DinoV2-small	DIMO: R	DIMO: Synth Counterpart	0.011015	0.025800	0.841786	0.697453
CLIP-ViT-B/32	RP: R Tr	RP: R Val	0.677107	0.729791	0.136138	0.119079
CLIP-ViT-B/32	RP: R Tr	RP: Synth	0.011446	0.021393	0.833652	0.729436
CLIP-ViT-B/32	W: R Tr	W: R Val	0.008366	0.017573	0.885283	0.760340
CLIP-ViT-B/32	W: R Tr	W: Synth	0.004075	0.009248	0.999894	0.862232
CLIP-ViT-B/32	DIMO: R	DIMO: Synth	0.052533	0.083358	0.589168	0.510899
CLIP-ViT-B/32	DIMO: R	DIMO: Synth Counterpart	0.005649	0.014801	0.947456	0.784795
GD text: "plane . aero- plane ."	RP: R Tr	RP: R Val	0.898451	0.913681	0.062346	0.056551
GD text: "plane . aero- plane ."	RP: R Tr	RP: Synth	0.085130	0.125567	0.507735	0.441276
GD text: "plane . aero- plane . jet . airplane . flight ."	RP: R Tr	RP: R Val	0.882684	0.899710	0.068129	0.061894
GD text: "plane . aero- plane . jet . airplane . flight ."	RP: R Tr	RP: Synth	0.065192	0.097946	0.550988	0.481972
GD text: "vehicle ."	W: R Tr	W: R Val	0.009586	0.019745	0.863149	0.741495
GD text: "vehicle ."	W: R Tr	W: Synth	0.006827	0.013952	0.917200	0.797097
GD text: "vehicle . car . jeep . truck ."	W: R Tr	W: R Val	0.010600	0.022013	0.846370	0.723660
GD text: "vehicle . car . jeep . truck ."	W: R Tr	W: Synth	0.004072	0.009397	0.999999	0.859747
GD text: "metal cube . rectangular tray . circu- lar metal piece . cylin- drical metal disc . metal rod . metal pipe ."	DIMO: R	DIMO: Synth	0.212445	0.285720	0.354814	0.301897
GD text: "metal cube . rectangular tray . circu- lar metal piece . cylin- drical metal disc . metal rod . metal pipe ."	DIMO: R	DIMO: Synth Counterpart	0.073652	0.120384	0.533366	0.448752

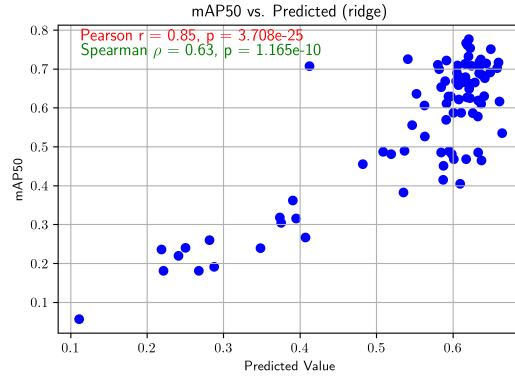


Fig 5 Validation datapoints with SDQM values calculated from ridge regression coefficients vs. YOLOv11n mAP50 scores.

less than random forest; however, we chose random forest due to its simplicity and robustness.

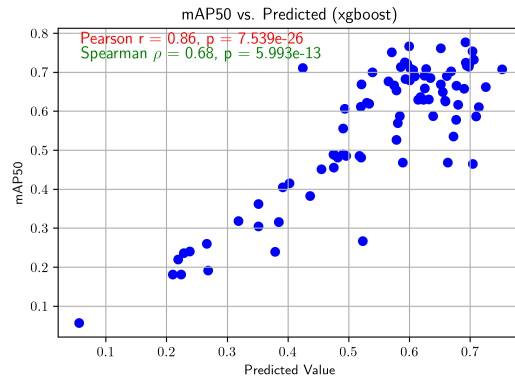


Fig 6 Validation datapoints with SDQM values calculated from XGBoost coefficients vs. YOLOv11n mAP50 scores.

Decision tree regression, displayed in Fig. 7 achieves adequate performance on our data. The added robustness of random forest achieved by introducing randomness may explain the deficit in the performance of decision tree regression.

Lasso regression, while showing promise over linear regression with an added regularization term, failed to capture any pattern in our data as shown in Fig 8.

Appendix E: Sub-Metric Regression Analysis

We perform quadratic analysis to combine sub-metrics into sub-components, removing terms with p-values greater than 0.05 for statistical significance. This reduces the number of terms needed.

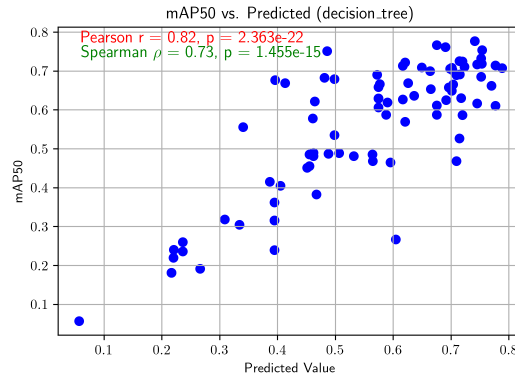


Fig 7 Validation datapoints with SDQM values calculated from decision tree coefficients vs. YOLOv11n mAP50 scores.

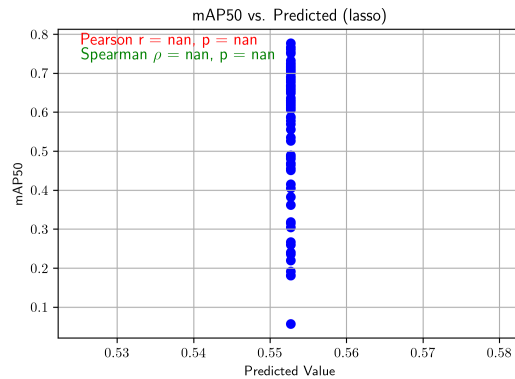


Fig 8 Validation datapoints with SDQM values calculated from lasso regression coefficients vs. YOLOv11n mAP50 scores.

For Bounding Box Match, after determining Energy Distance to be the most effective statistical method for comparison based on p-values, we analyze the remaining sub-components. Removing sub-components from the regression used for combination with a p-value greater than 0.05, we are left with the Energy Distance between aspect ratio, size, and area distributions. Also left included are the square of the aspect ratio and size comparisons, as well as the interaction term between aspect ratio and size comparisons.

Applying the same process to the regression of the sub-components of Pixel Intensity Match after A-D Statistic was selected, the green pixel-value sub-component and square of the red pixel-value sub-component along with the interaction term between them is left. The blue pixel-value

terms were completely removed, suggesting the blue-pixel value match is not as important for predicting mAP.

The last of the sub-metrics utilizing non-parametric statistical methods, Label Overlap, contains only one sub-component. Our regression analysis determined the square of the K-S Statistic value was the most useful variable for this sub-metric.

MAUVE, which was dropped from the final metric, consists of MAUVE and MAUVE*—the latter being a smoothed version. We use $(\text{MAUVE}^*)^2 + (\text{MAUVE})(\text{MAUVE}^*)$ to combine these sub-components. We found that Frontier Integral, which correlated highly with MAUVE, was most effective with only its smoothed variant as a single linear term.

Clusterability (removed from the final SDQM metric), consisting of sub-components with (l) and without (c) a logarithm applied, reduced to the following regression equation: $c^2 + l^2 + cl + c + l$.

\mathcal{V} -Information, the sub-metric with the highest correlation with mAP50, reduced to Predictive Confidence, Conditional Fusion, and the interaction term between IoU \mathcal{V} -Information and Conditional Fusion.

Sub-metrics with only one sub-component, denoted x , include Spatial Distribution Difference, α -Precision, β -Recall, and Authenticity (Authenticity was removed from the final metric). All besides α -Precision, which uses a single linear term, use a linear term and a quadratic term $(x + x^2)$.

Disclosures

We acknowledge that there are no conflicts to declare.

Code and Data Availability

The code used in our study is publicly available at <https://github.com/ayushzenith/SDQM>.

The WASABI dataset can be requested from the corresponding author. The DIMO dataset is accessible at <https://pderoovere.github.io/dimo>, and RarePlanes can be found at <https://www.iqt.org/library/the-rareplanes-dataset>.

Acknowledgments

We acknowledge the AFRL Internship Program to support Ayush Zenith, Arnold Zumbrun, and Neel Raut's work. This material is based upon work supported by the Air Force Research Laboratory under agreement number FA8750-20-3-1004. Any opinions, findings, conclusions, or recommendations expressed in this publication are those of the authors and do not necessarily reflect the views of the U.S. Air Force. The U.S. Government is authorized to reproduce and distribute reprints for Governmental purposes notwithstanding any copyright notation thereon.

References

- 1 J. Shermeyer, T. Hossler, A. Van Etten, *et al.*, “Rareplanes: Synthetic data takes flight,” in *Proceedings of the IEEE/CVF Winter Conference on Applications of Computer Vision*, 207–217 (2021). [doi:10.48550/arXiv.2006.02963].
- 2 P. D. Roovere, S. Moonen, N. Michiels, *et al.*, “Dataset of industrial metal objects,” *CoRR abs/2208.04052* (2022). [doi:10.48550/arXiv.2208.04052].
- 3 M. A. Esposito, J. Lin, R. Young, *et al.*, “Odusi: object detection using synthetic imagery,” in *Synthetic Data for Artificial Intelligence and Machine Learning: Tools, Techniques, and Applications II*, **13035**, 322–332, SPIE (2024). [doi:10.1117/12.3013516].

- 4 Z. Wang, A. C. Bovik, H. R. Sheikh, *et al.*, “Image quality assessment: from error visibility to structural similarity,” *IEEE Trans. Image Process.* **13**(4), 600–612 (2004). [doi:10.1109/TIP.2003.819861].
- 5 R. Zhang, P. Isola, A. A. Efros, *et al.*, “The unreasonable effectiveness of deep features as a perceptual metric,” in *2018 IEEE Conference on Computer Vision and Pattern Recognition, CVPR 2018, Salt Lake City, UT, USA, June 18-22, 2018*, 586–595, Computer Vision Foundation / IEEE Computer Society (2018). [doi:10.1109/CVPR.2018.00068].
- 6 T. Salimans, I. J. Goodfellow, W. Zaremba, *et al.*, “Improved techniques for training gans,” in *Advances in Neural Information Processing Systems 29: Annual Conference on Neural Information Processing Systems 2016, December 5-10, 2016, Barcelona, Spain*, D. D. Lee, M. Sugiyama, U. von Luxburg, *et al.*, Eds., 2226–2234 (2016).
- 7 M. Heusel, H. Ramsauer, T. Unterthiner, *et al.*, “Gans trained by a two time-scale update rule converge to a local nash equilibrium,” in *Advances in Neural Information Processing Systems 30: Annual Conference on Neural Information Processing Systems 2017, December 4-9, 2017, Long Beach, CA, USA*, I. Guyon, U. von Luxburg, S. Bengio, *et al.*, Eds., 6626–6637 (2017).
- 8 A. Borji, “Pros and cons of GAN evaluation measures: New developments,” *Comput. Vis. Image Underst.* **215**, 103329 (2022). [doi:10.1016/j.cviu.2021.103329].
- 9 K. Pillutla, L. Liu, J. Thickstun, *et al.*, “MAUVE scores for generative models: Theory and practice,” *J. Mach. Learn. Res.* **24**, 356:1–356:92 (2023).
- 10 T. Kynkäänniemi, T. Karras, S. Laine, *et al.*, “Improved precision and recall metric for assessing generative models,” in *Advances in Neural Information Processing Systems 32: Annual*

- Conference on Neural Information Processing Systems 2019, NeurIPS 2019, December 8-14, 2019, Vancouver, BC, Canada*, H. M. Wallach, H. Larochelle, A. Beygelzimer, *et al.*, Eds., 3929–3938 (2019).
- 11 A. M. Alaa, B. van Breugel, E. S. Saveliev, *et al.*, “How faithful is your synthetic data? sample-level metrics for evaluating and auditing generative models,” in *International Conference on Machine Learning, ICML 2022, 17-23 July 2022, Baltimore, Maryland, USA*, K. Chaudhuri, S. Jegelka, L. Song, *et al.*, Eds., *Proceedings of Machine Learning Research* **162**, 290–306, PMLR (2022).
 - 12 K. Ethayarajh, Y. Choi, and S. Swayamdipta, “Understanding dataset difficulty with V-usable information,” in *International Conference on Machine Learning, ICML 2022, 17-23 July 2022, Baltimore, Maryland, USA*, K. Chaudhuri, S. Jegelka, L. Song, *et al.*, Eds., *Proceedings of Machine Learning Research* **162**, 5988–6008, PMLR (2022).
 - 13 S. Swayamdipta, R. Schwartz, N. Lourie, *et al.*, “Dataset cartography: Mapping and diagnosing datasets with training dynamics,” in *Proceedings of the 2020 Conference on Empirical Methods in Natural Language Processing, EMNLP 2020, Online, November 16-20, 2020*, B. Webber, T. Cohn, Y. He, *et al.*, Eds., 9275–9293, Association for Computational Linguistics (2020). [doi:10.18653/v1/2020.emnlp-main.746].
 - 14 J. Djolonga, M. Lucic, M. Cuturi, *et al.*, “Precision-recall curves using information divergence frontiers,” in *The 23rd International Conference on Artificial Intelligence and Statistics, AISTATS 2020, 26-28 August 2020, Online [Palermo, Sicily, Italy]*, S. Chiappa and R. Calandra, Eds., *Proceedings of Machine Learning Research* **108**, 2550–2559, PMLR (2020).

- 15 H. Jin, F. Chollet, Q. Song, *et al.*, “Autokeras: An automl library for deep learning,” *Journal of Machine Learning Research* **24**(6), 1–6 (2023).
- 16 G. Fasano and A. Franceschini, “A multidimensional version of the kolmogorov–smirnov test,” *Monthly Notices of the Royal Astronomical Society* **225**(1), 155–170 (1987). [doi:10.1093/mnras/225.1.155].
- 17 M. Arshad, M. Rasool, and M. Ahmad, “Anderson darling and modified anderson darling tests for,” *Pakistan Journal of Applied Sciences* **3**(2), 85–88 (2003). [doi:10.3923/jas.2003.85.88].
- 18 S. Kullback and R. A. Leibler, “On information and sufficiency,” *The annals of mathematical statistics* **22**(1), 79–86 (1951). [doi:10.1214/aoms/1177729694].
- 19 M. L. Rizzo and G. J. Székely, “Energy distance,” *wiley interdisciplinary reviews: Computational statistics* **8**(1), 27–38 (2016). [doi:10.1002/wics.1375].
- 20 C. Villani *et al.*, *Optimal transport: old and new*, vol. 338, Springer (2009). [doi:10.1007/978-3-540-71050-9].
- 21 A. Bhattacharyya, “On a measure of divergence between two statistical populations defined by their probability distribution,” *Bulletin of the Calcutta Mathematical Society* **35**, 99–110 (1943).
- 22 J. Lin, “Divergence measures based on the shannon entropy,” *IEEE Transactions on Information theory* **37**(1), 145–151 (1991). [doi:10.1109/18.61115].
- 23 G. Jocher and J. Qiu, “Ultralytics yolo11,” (2024).
- 24 T. Lin, M. Maire, S. J. Belongie, *et al.*, “Microsoft COCO: common objects in context,” in *Computer Vision - ECCV 2014 - 13th European Conference, Zurich, Switzerland, September*

- 6-12, 2014, *Proceedings, Part V*, D. J. Fleet, T. Pajdla, B. Schiele, *et al.*, Eds., *Lecture Notes in Computer Science* **8693**, 740–755, Springer (2014). [doi:10.1007/978-3-319-10602-1_48].
- 25 M. Oquab, T. Darcet, T. Moutakanni, *et al.*, “Dinov2: Learning robust visual features without supervision,” *Trans. Mach. Learn. Res.* **2024** (2024).
- 26 S. Liu, Z. Zeng, T. Ren, *et al.*, “Grounding DINO: marrying DINO with grounded pre-training for open-set object detection,” *CoRR* **abs/2303.05499** (2023). [doi:10.48550/arXiv.2303.05499].
- 27 A. Radford, J. W. Kim, C. Hallacy, *et al.*, “Learning transferable visual models from natural language supervision,” in *Proceedings of the 38th International Conference on Machine Learning, ICML 2021, 18-24 July 2021, Virtual Event*, M. Meila and T. Zhang, Eds., *Proceedings of Machine Learning Research* **139**, 8748–8763, PMLR (2021).
- 28 R. Kohavi and G. H. John, “Wrappers for feature subset selection,” *Artif. Intell.* **97**(1-2), 273–324 (1997). [doi:10.1016/S0004-3702(97)00043-X].
- 29 F. Hayes-Roth, “Review of ”adaptation in natural and artificial systems by john h. holland”, the u. of michigan press, 1975,” *SIGART Newsl.* **53**, 15 (1975). [doi:10.1145/1216504.1216510].

List of Figures

- 1 Correlation between each sub-metric and mAP50.
- 2 WASABI object size and count. Note: “Small,” “Medium,” and “Large” definitions are based on Ref. 24.

- 3 Validation datapoints with SDQM values calculated from random forest coefficients vs. YOLOv11n mAP50 scores.
- 4 Validation datapoints with SDQM values calculated from linear regression coefficients vs. YOLOv11n mAP50 scores.
- 5 Validation datapoints with SDQM values calculated from ridge regression coefficients vs. YOLOv11n mAP50 scores.
- 6 Validation datapoints with SDQM values calculated from XGBoost coefficients vs. YOLOv11n mAP50 scores.
- 7 Validation datapoints with SDQM values calculated from decision tree coefficients vs. YOLOv11n mAP50 scores.
- 8 Validation datapoints with SDQM values calculated from lasso regression coefficients vs. YOLOv11n mAP50 scores.

List of Tables

- 1 Description of all parameters, functions, and variables in Algorithm 1.
- 2 Correlation of alternative metrics and SDQM with mAP50 scores.
- 3 Feature extraction model evaluation report.
- 4 α -Precision, β -Recall, and Authenticity scores of the various synthetic and real-world dataset pairs.
- 5 MAUVE and Frontier Integral scores (along with smoothed variants indicated by *) of the various synthetic and real-world dataset pairs.